Journal of Materials Chemistry C

Accepted Manuscript

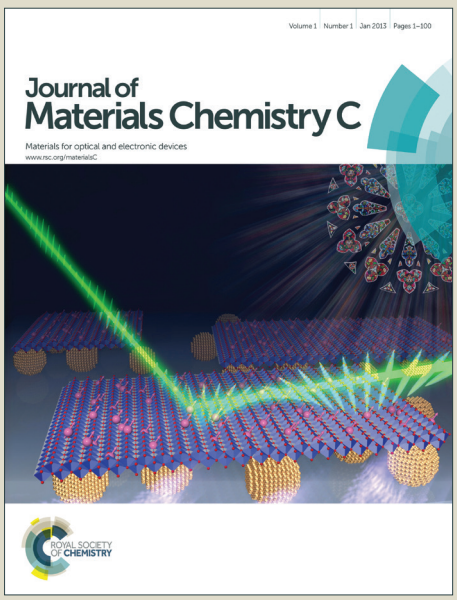

ROYAL SOCIETY OF CHEMISTRY

www.rsc.org/materialsC

Journal Name

RSCPublishing

ARTICLE

Design of indigo derivatives as environment-friendly organic semiconductors for sustainable organic electronics

Cite this: DOI: 10.1039/x0xx00000x

Received 00thMarch 2014,
Accepted 00th January 2012

DOI: 10.1039/x0xx00000x

www.rsc.org/

I. V. Klimovich,[a] L. I. Leshanskaya,[a] S. I. Troyanov,[b] D. V. Anokhin,[a,c] D. V. Novikov,[a,d] A. A. Piryazev,[c] D. A. Ivanov,[c,e] N. N. Dremova,[a] and P. A. Troshin[a*]

We report the synthesis and systematic investigation of nine different indigo derivatives as promising materials for sustainable organic electronics. It has been shown that chemical design allows one to tune optoelectronic properties of indigoids as well as their semiconductor performance in OFETs. Fundamental correlations between the molecular structures of indigo derivatives, structural characteristics of their films, charge carrier transport properties and transistor characteristics have been revealed. Particularly important was lowering the LUMO energy levels of indigoids bearing strong electron withdrawing groups which improved dramatically ambient stability of n-type OFETs. Chemical structures of novel indigoids enabling truly air-stable n-channel OFET operation were proposed.

Introduction

Rapid scientific and technological progress attained in the field of organic electronics within the last decade resulted in commercialization of a number of innovative products, currently dominated by OLED displays.[1] It is generally believed that the next commercial products will be based on simple electronic logics composed of organic field-effect transistors (OFETs).A niche of single-use applications produced in extremely large volumes (e.g. smart food packaging, RFID tags and cards, tickets and etc.) will be particularly pursued.[2] However, massive production and use of disposable plastic electronics might cause severe pollution effects in the environment.[3] This problem might be solved via design and implementation of biodegradable or biocompatible electronics which is based entirely on environment-friendly non-toxic materials. This approach was pursued by M. Irimia-Vladu in collaboration with our group.[4-5]

Indigoids represent a family of organic compounds which have very low acute toxicity and are widely used as textile dyes, food colorants and pigments for contact lenses.[6] The application of ancient organic dye indigo and its derivatives as organic semiconductors was first proposed in a Japanese patent application filed in 2006.[7] Later on indigo was shown to be one of the most promising biocompatible semiconductor materials exhibiting balanced ambipolar transport in OFETs and good performance in inverter circuits.[4,8] Other indigoid, 6,6'-dibromoindogo known as Tyrian purple dye also demonstrated ambipolar behavior in OFETs.[9] Recently, two other halogenated indigo derivatives (6,6'-dichloroindigo and 5-bromoindigo) were preliminary presented in a review paper as promising ambipolar semiconductor materials for OFETs.[10] Particularly intriguing was an excellent ambient operation stability reported for ambipolar indigoid-based OFETs.[9-10]Low toxicity of indigo and its derivatives, natural occurrence of some indigoids in combination with good semiconductor characteristics and chemical stability open wide opportunities for their use in the development of sustainable electronics.

We have shown recently that electrical performance of pristine indigo can be enhanced using a strong template effect of aliphatic hydrocarbon dielectrics.[11] In the present work we explored a potential of chemical derivatization of indigo as a route for designing indigoid-based semiconductors with advanced properties. Nine different indigo derivatives were synthesized and investigated in order to identify fundamental correlations between the molecular structures of compounds, their crystal packing, film morphology, optical, electrochemical and electrical properties as well as operational stability under ambient conditions.

Results and discussion

We intentionally pursued indigo derivatives modified with electron withdrawing groups such as halogen atoms, CN and CF_3. Introducing electron deficient substituents is expected to lower the LUMO energy levels of these molecules compared to the parent indigo. Such modification should lead to an

improved stability of their anion species required for a stable n-channel OFET operation under ambient conditions.

The target indigo derivatives were synthesized using corresponding substituted 2-nitrobenzaldehydes as precursors which were treated with nitromethane and MeONa according to the Scheme 1. The starting aldehydes were obtained by oxidation of the substituted 2-nitrotoluenes using dimethylformamide dimethyl acetal – sodium periodate system or by lithiation of 1-bromo-2-nitrobenzenes with PhLi and subsequent quenching of the formed intermediate with DMF according to the previously described general procedures.[12] The latter method was not efficient in the case of compound **5** (yield 36%) presumably because of the involvement of the electrophilic CN group in the reaction with the nucleophilic lithiated intermediate. On the contrary, 2-nitrotoluene route was found to be equally efficient in all cases enabling the preparation of various indigo derivatives on a larger scale.

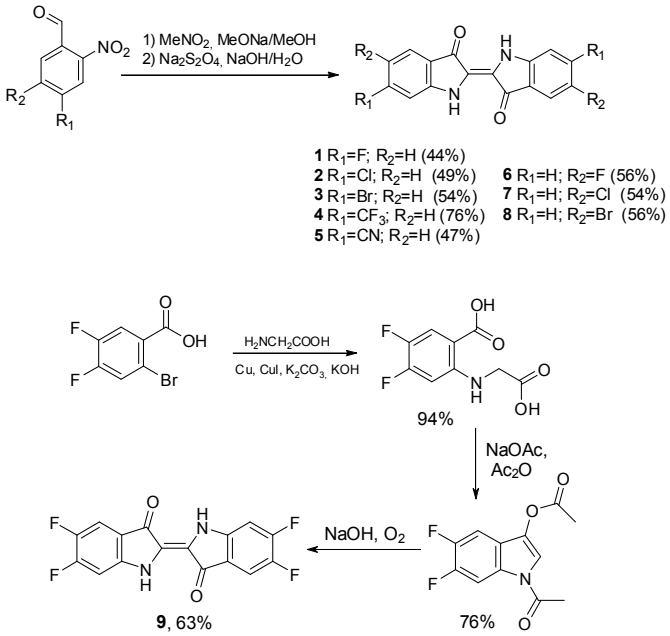

Scheme 1 Synthesis of indigo derivatives

The corresponding toluene precursor for synthesis of 5,5',6,6'-tetrafluoroindigo was not available. Therefore, the compound **9** was synthesized from 2-bromo-4,5-difluorobenzoic acid in three steps with acceptable yields (Scheme 1) following another route reported in the literature.[13]

All synthesized indigo derivatives were obtained as dark blue or violet powders which were hardly soluble in any organic solvent at ambient conditions. Therefore, their NMR characterization in solution turned to be almost impossible. However, most of the synthesized compounds were sufficiently soluble in DMF and acetonitrile to confirm their molecular compositions using ESI MS spectroscopy. FTIR spectra of indigoids **1-3** and **6-8** corresponded to the literature data.[14] The FTIR spectra of new compounds **4** and **9** as well as previously known but non-sufficiently characterized compound **5** were in a full agreement with their molecular structures. Chemical analysis data obtained for compounds **1-9** also supported their compositions and structures (see ESI).

All indigoids exhibit very characteristic absorption spectra which are known to be very sensitive to the electronic nature of the introduced substituents and their positions in the indigo core.[15] Indeed, all compounds demonstrated rather different optical spectra measured for their solutions in hot 1,2-dichlorobenzene (Fig. 1) and thin films (Electronic supplementary information, ESI, Fig. S2). In a full accordance with the literature data,[15] 6,6'-dihalogenated indigoids showed hypsochromic shifts in comparison with the parent indigo and magnitude of these shifts becomes bigger with increased electronegativity of the halogen substituents: **1**(F)>**2**(Cl)>**3**(Br). The hypsochromic shifts of the absorption bands of indigoids **1-3** *vs*. parent indigo observed in solution become even more pronounced when going to thin films (Fig. 1b, Table 1), which suggests that formation of H-aggregates[16] might be responsible for such behavior.

Strongly electron deficient non-halogen substitutents such as CF_3 (**4**) and CN (**5**) afforded small (**4**) or substantial (**5**) bathochromic shifts similarly to 6,6'-dinitroindigo reported previously.[15] At the same time, halogen substituents introduced in 5 and 5' positions of indigo core induced weak bathochromic shifts and their magnitude also increases with increase in the electronegativity of the halogen atom **8**(Br)<**7**(Cl)<**6**(F).

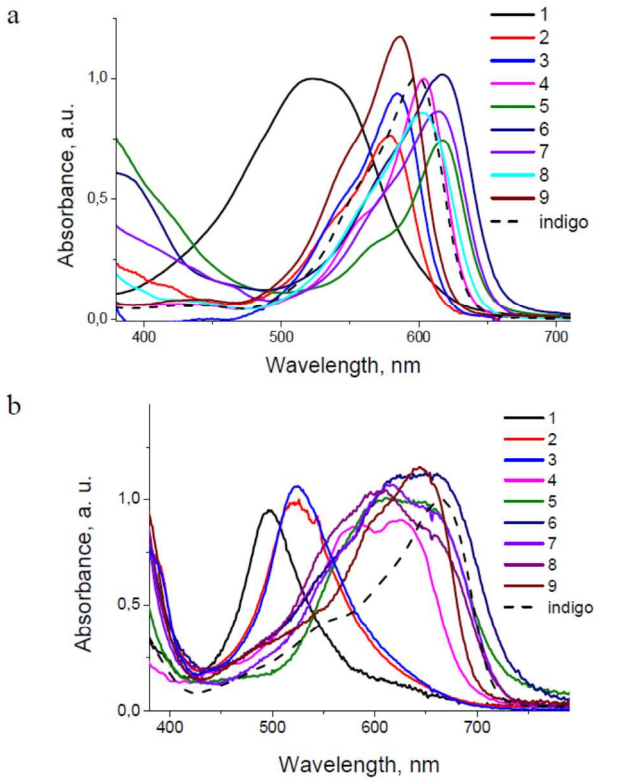

Figure 1. Visible-range absorption spectra of indigo derivatives **1-9** in 1,2-dichlorobenzene (a) and in solid films (b). Full spectra are given in Figs. S1-S2, ESI

The case of tetrafluoroindigo **9** is rather specific since it contains fluorine substituents in positions 5 and 5' as well as 6 and 6' which cause opposite electronic effects. Therefore, the absorption band of **9** has its maximum at 586 nm which lies in between the maxima of the bands of bisfluorinated compounds **1** (525 nm) and **6** (618 nm). The observed bathochromic and hypsochromic shifts of the absorption bands of indigoids **1-9** *vs*. parent indigo in solution become even more pronounced when going to thin films (Fig. S2, Table 1).

Cyclic voltammetry measurements were performed for thin films of **1-9** deposited by thermal evaporation on glassy carbon disc electrodes to reveal onsets of the oxidation and reduction waves for these compounds. A standard approach described in the literature[17] was also used to estimate HOMO and LUMO energies of the investigated indigoids based on their electrochemical properties using the Fermi energy of -5.1 eV for the Fc^+/Fc redox couple. The obtained data are summarized in Table 1. It is seen from the table and Figs. S3-S4 (ESI) that introducing chlorine and bromine atoms to the indigo core affects mostly HOMO energies of the resulting compounds, while their LUMO levels remain unchanged compared to parent indigo. Such behavior can be explained by the fact that LUMO in indigo is localized mostly on the carbonyl groups and, therefore, it should not be very sensitive to the substitution in the benzene rings.

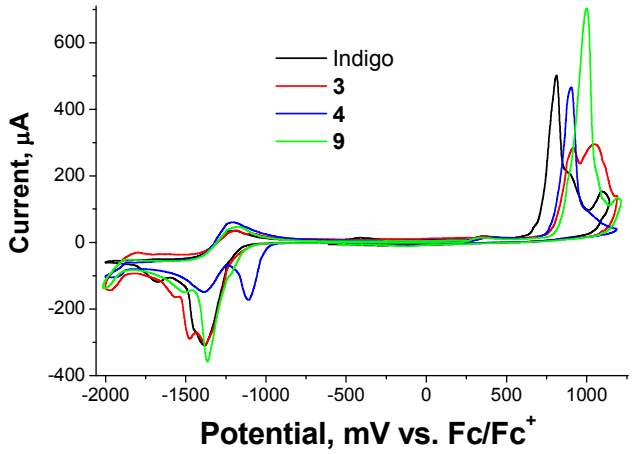

Figure 2. Cyclic voltammograms of the parent indigo and some representative indigoids

It is somewhat surprising that 6,6'-difluoroindogo **1** shows the same electrochemical properties as indigoids bearing two chlorine (**2**) or bromine (**3**) substituents (Fig. S3). However, fluorine substitution at the positions 5 and 5' induces different electronic effects: HOMO energy of the resulting compound **6** remains equal to that of unsubstituted indigo, while LUMO energy is decreased by ~100 meV down to -3.97 eV (Fig. S4, Table 1).

The increased reduction potentials correlated with the decreased LUMO energy levels are observed for indigoids bearing strongly electron withdrawing groups such as CF_3- and CN- (Fig. 2). It is seen from the table 1 that compounds **4** and **5** have ca. 200 mV lower LUMO energies compared to the parent indigo. This behavior resembles closely 6,6'-dinitroindigo which also possesses two electron withdrawing nitro groups.[15-16] Most probably, the polarization induced by the electron deficient substituents changes localization of LUMO towards benzene rings. Similar explanation was provided in the literature based on the resonance theory.[15]

Table 1 Optical and electrochemical properties of **1-9** and parent indigo

No	λ_{max} sol., nm	λ_{max}film,nm	E_g film, eV	$E^{ox}_{ons.}$ V *vs.* Fc/Fc^+	HOMO eV	$E^{red}_{ons.}$ V *vs.* Fc/Fc^+	LUMO eV	E_g El. eV
1	525	498	2.06	0.78	-5.88	-1.20	-3.90	1.98
2	579	529	1.94	0.78	-5.88	-1.20	-3.90	1.98
3	583	526	1.93	0.78	-5.88	-1.20	-3.90	1.98
4	604	587, 626	1.76	0.75	-5.85	-1.00	-4.10	1.75
5	617	612, 650	1.67	0.80	-5.90	-0.96	-4.14	1.76
6	618	625, 657	1.64	0.67	-5.77	-1.13	-3.97	1.80
7	614	614, 657	1.70	0.73	-5.83	-1.19	-3.91	1.92
8	603	605, 653	1.70	0.73	-5.83	-1.20	-3.90	1.93
9	586	643	1.75	0.82	-5.92	-1.13	-3.97	1.95
I*	600	665	1.71	0.67	-5.77	-1.20	-3.90	1.87

* "**I**" corresponds to the parent indigo

Summarizing the obtained results, we can conclude that it is indeed possible to lower LUMO energy of indigoids by chemical design using strongly electron deficient substituents such as CN, CF_3 and NO_2. At the same time, introducing two or even four fluorine atoms leads to relatively small decrease in the LUMO energy levels of the corresponding indigoids.

The indigoids **1-9** were investigated as semiconductor materials in organic field-effect transistors which had an architecture shown in Fig. 3. It is known that use of AlO_x as gate dielectric provides for low operation voltages of the devices.[2]

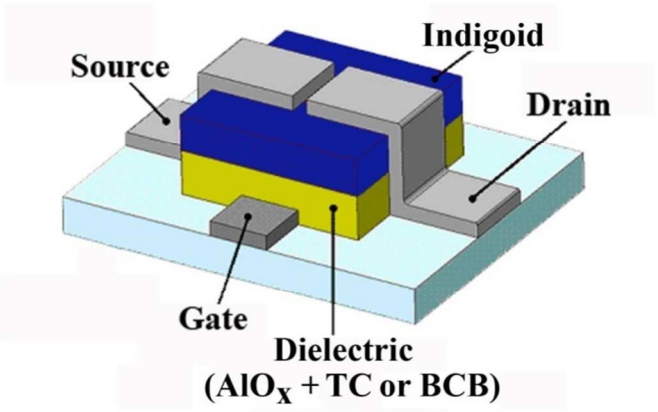

Figure 3 General layout of the OFET

To fabricate these devices, aluminum gate electrodes were subjected to anodic oxidation (anodization) in a citric acid

solution using potentiostatic regime (10 V). The anodized electrodes were washed with deionized water and dried in air. Afterwards, an organic dielectric coating was applied by spin-coating. We have shown recently that aliphatic hydrocarbon dielectrics serve as templates modifying the crystal structure of indigo and improving charge transport properties of this material. Therefore, in this work we also investigated two types of dielectric coatings: normal-chain hydrocarbon tetracontane ($C_{40}H_{82}$, TC) and a cross-linked benzocyclobutene derivative (BCB). We emphasize that we did not apply a hot wall epitaxial growth (HWEG) for deposition of semiconductor films like it was done in the previous studies.[8-9] On the one hand, simple thermal evaporation of the semiconductor materials on a non-heated rotating substrate results in less crystalline films which show lower charge carrier mobilities compared to the films obtained using HWEG. However, simple thermal evaporation technique allows for processing all materials under very similar conditions which is a strong advantage for purpose of their direct comparison.

Table 2 Characteristics of OFETs comprising indigo and its derivatives as semiconductors, TC or BCB as organic dielectric coatings and gold source and drain electrodes

Comp.	type	Diel.	V_{TH}	I_{on}/I_{off}	μ, $cm^2V^{-1}s^{-1}$	μ_e/μ_h (TC)
1	n	BCB	4.0	$2\cdot10^3$	$(2.0\text{-}2.4)\cdot10^{-3}$	n/a
	n	TC	3.7	$5\cdot10^3$	$(0.9\text{-}1.0)\cdot10^{-2}$	~22
	p	TC	-6.6	$1\cdot10^2$	$(3.6\text{-}4.5)\cdot10^{-4}$	
2	n	BCB	1.8	$9\cdot10^3$	$(5.0\text{-}6.0)\cdot10^{-3}$	n/a
	n	TC	3.1	$2\cdot10^4$	$(1.1\text{-}1.3)\cdot10^{-2}$	~10
	p	TC	-6.0	$1\cdot10^2$	$(0.9\text{-}1.3)\cdot10^{-3}$	
3	n	BCB	3.2	$1\cdot10^2$	$(5.0\text{-}6.2)\cdot10^{-4}$	
	n	TC	2.6	$1\cdot10^4$	$(7.0\text{-}9.0)\cdot10^{-3}$	~4
	p	TC	-3.0	$1\cdot10^3$	$(1.8\text{-}2.1)\cdot10^{-3}$	
4	n	BCB	-	-	-	n/a
	n	TC	1.0	$8\cdot10^2$	$(2.3\text{-}2.8)\cdot10^{-3}$	∞
	p	TC	-	-	-	
5	n	BCB	-	-	-	n/a
	n	TC	-	-	-	n/a
	p	TC	-	-	-	
6	n	BCB	-	-	-	n/a
	n	TC	4.0	$4\cdot10^2$	$(1.7\text{-}2.1)\cdot10^{-4}$	∞
	p	TC	-	-	-	
7	n	BCB	4.1	$2\cdot10^2$	$(1.3\text{-}2.5)\cdot10^{-4}$	n/a
	n	TC	2.3	$2\cdot10^3$	$(0.9\text{-}1.2)\cdot10^{-3}$	~7
	p	TC	-4.3	$5\cdot10^2$	$(1.0\text{-}1.8)\cdot10^{-4}$	
8	n	BCB	3.7	100	$(4.3\text{-}7.7)\cdot10^{-5}$	n/a
	n	TC	3.2	50	$(2.0\text{-}4.1)\cdot10^{-5}$	∞
	p	TC	-	-	-	
9	n	BCB	0.4	$1\cdot10^3$	$(1.6\text{-}2.2)\cdot10^{-3}$	n/a
	n	TC	0.7	$3\cdot10^3$	$(4.7\text{-}5.9)\cdot10^{-3}$	∞
	p	TC	-	-	-	
indigo	n	BCB	3.8	$3\cdot10^2$	$(0.8\text{-}1.5)\cdot10^{-4}$	n/a
	n	TC	4.9	$4\cdot10^3$	$(1.0\text{-}1.3)\cdot10^{-3}$	~4
	p	TC	-5.0	$2\cdot10^2$	$(1.0\text{-}3.0)\cdot10^{-4}$	

symbol "-" means that no transistor behavior was observed

The OFET devices were finalized with the deposition of source and drain electrodes. The OFETs fabricated using silver top electrodes demonstrated only n-type behavior and their characteristics are given in Tables S1 and S2 (ESI). Using gold electrodes was favorable for both p-type and n-type transport and parameters of these devices are summarized in Table 2 (transfer and output characteristics are given in Table S3, ESI).

The data presented in Table 2 show clearly that chemical modification of indigo affects strongly the electrical performance of the resulting indigo derivatives. In general, 6,6'-disubstituted indigoids **1-3** outperform significantly their 5,5'-disubstituted analogues **6-8**. The best performing 5,5'-dichloroindigo **7** showed *ca*. 10 times lower electron mobility compared to 6,6'-dichloroindigo **2**. This difference becomes larger and approaches 2-3 orders of magnitude for compounds bearing two fluorine or two bromine atoms as substituents. Noteworthy is also the fact that only compound **7** showed ambipolar behavior in OFETs among three studied 5,5'-disubstituted indigo derivatives.

Halogen-substituted indigoids **1-3** showed very similar electron mobilities which exceed by one order of magnitude the electron mobility in parent indigo (Table 2). The hole mobilities decreased in parallel with the increased electronegativity of the substituents introduced to the indigo molecule as it is illustrated by the Fig. 4. Therefore, the most balanced ambipolar transport is delivered by 6,6-dibromoindigo **3**, while compounds **4** and **9** bearing electron deficient substituents exhibited purely n-type behavior.

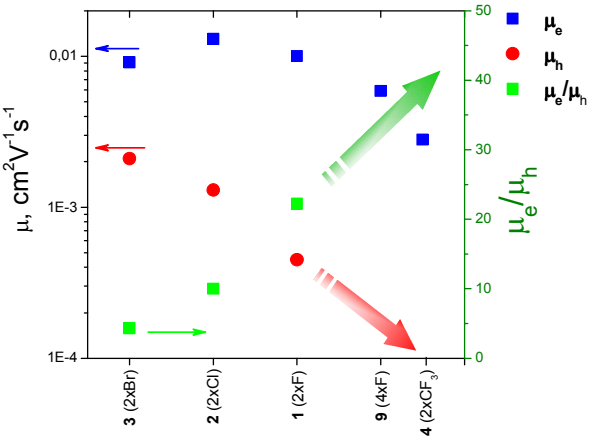

Figure 4 Change of the OFET hole and electron mobilities in indigo derivatives upon the chemical functionalization

It is reasonable to assume that the presence of electron withdrawing substituents such as Cl, F or CF_3 in the indigo core increases the barrier for the hole injection and facilitates the electron injection. This assumption is tentatively supported by the threshold voltages (V_{TH}) given in the Table 2. Indeed, the 6,6'-dibromoindigo **3** showed the lowest V_{TH} in p-channel OFETs, while 6,6'-bis(trifluoromethyl)indigo **4** and 5,5',6,6'-tetrafluoroindigo **9** revealed the lowest V_{TH} in n-type devices. Therefore, we believe that the observed decrease of the hole mobilities in the raw **3** > **2** > **1** might be related to increased barriers for injection of the positive charge carriers. At the same time, increased hole injection barrier correlates well with the decreased stability of the respective cation species as can be

concluded on the basis of the previously reported effects of the resonance stabilization of indigoids.[15]

The influence of the dielectric material on the structure and properties of semiconductor is other important issue which has to be considered in more detail. In order to compare electrical characteristics of OFETs comprising different organic dielectric coatings we introduced two parameters: the ratio of the electron mobilities μ_e(TC)/μ_e(BCB) and the corresponding currents ratio [I_{on}/I_{off}(TC)]/[I_{on}/I_{off}(BCB)]. It is seen from the Table 2 that OFETs comprising TC as organic dielectric coating typically outperform analogous devices where BCB was used for the same purpose. However, the magnitude of this effect changes significantly going from one indigoid to another. The transfer characteristics of OFETs comprising semiconductor layers of 5,5'6,6'-tetrafluoroindigo **9** and 6,6'-bis(trifluoromethyl)indigo **4** grown on TC or BCB are shown in Figure 5. It is seen from the figure that indigoid **9** exhibits comparable performances on both dielectric coatings. On the contrary, the films of compound **4** perform well on TC and do not show any transistor behavior on BCB. The observed sharply different behavior of the investigated indigoids allows one to divide them in two groups: the materials which are highly sensitive to the type of the dielectric (μ_e(TC)/μ_e(BCB)>5; compounds **3**, **4** and parent indigo) and the materials which perform similarly on both dielectric coating (**1**, **2**, **7**, **8**, **9**).

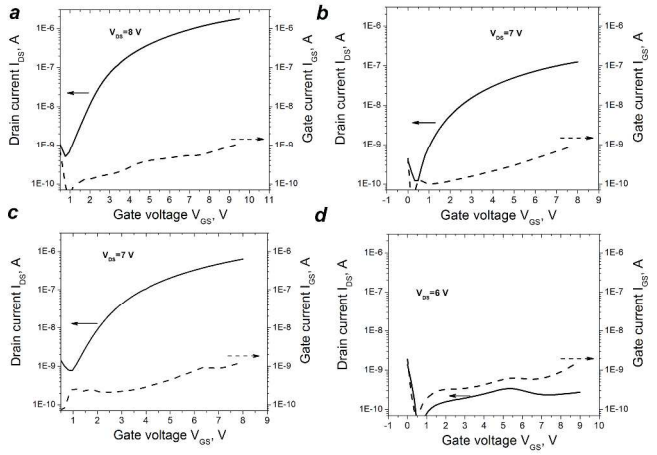

Figure 5. Transfer characteristics of OFETs based on indigoids **9** (a, b) and **4** (c, d) and comprising TC (a, c) and BCB (b, d) dielectricts given in the same scale for purpose of comparison.

Different morphology of the semiconductor films deposited on different dielectric underlayers has to be considered as a possible factor influencing the performance of OFETs.[18] The films of all nine indigoids grown on TC and BCB dielectric coatings were investigated using atomic force microscopy (AFM) and scanning electron microscopy (SEM). Indeed, it was revealed that the surface topography of the films grown on BCB and TC might be very different for some materials (Fig. 6, Tables S4 and S5, ESI).

However, the changes in the surface topography of the films failed to explain the observed differences in the electrical performance of OFETs fabricated using the same semiconductor and different dielectrics (TC or BCB). For instance, indigoid **2** shows much more crystalline films when it is deposited on TC rather than on BCB (Fig. 6). However, the electrical performances of both types of films are very comparable (Table 2). At the same time, indigoid **3** shows very similar morphology of the films deposited on BCB and TC, while their performances in OFETs are drastically different. Similar observations can be made also for other indigoids (see Tables S4 and S5, ESI). Therefore, the bulk morphology of the semiconductor films cannot be directly correlated with the effects of underlying dielectric coatings on the characteristics of OFETs.

Recently we showed that aliphatic hydrocarbon dielectrics such as TC serve as templates which induce serious changes in the crystal structure of indigo in the adjacent layers leading to its advanced performance in OFETs.[11] It is possible that similar effects also play a role in the case of indigoids **1**-**9**. To verify this hypothesis, one has to compare the real 3D crystal structures of indigoids (bulk structures) with the structures of polymorphs formed in thin films at the semiconductor/dielectric interface (surface structures).

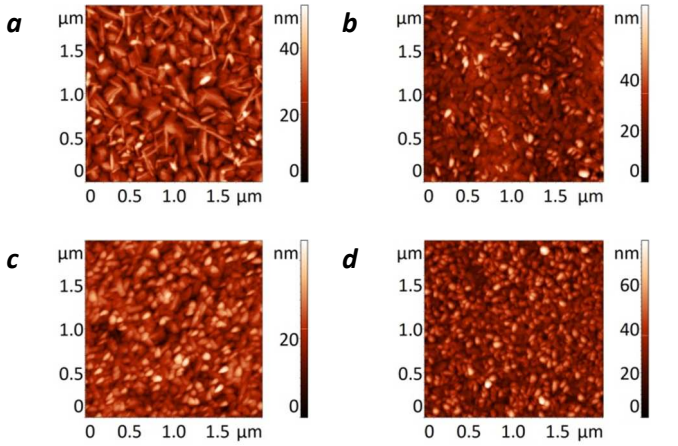

Figure 6 AFM images of thin films of **2** (a, b) and **3** (c, d) grown on TC (a, c) and BCB (b,d)

The bulk structures of indigoids **1**, **4**, **6**, **7** and **9** were determined in this work using x-ray single crystal diffraction. The crystal structures of parent indigo and indigoids **2** and **3** are known from the literature.[19] Figure 7 shows the arrangements of molecules in the π-stacks of different indigoids as revealed for their crystals. In the case of some indigoids the neighboring molecules in the stack are strongly shifted with respect to each other which is very typical of J-aggregates. The shift can be quantified by measuring the angle ω between the equal groups of the neighboring molecules and one of their plains (zero shift corresponds to the angle ω=90°, Fig. S5, ESI). In the case of the parent indigo and indigioids **1** and **6** this angle approaches ~145-147 degrees. However, it is significantly reduced to ~130 degrees for indigoids **3**, **7** and **9**. The structure of 6,6'-dicloroindigo **2** is rather remarkable since in this case the ω is

very close to 90° which means that the molecules are virtually not shifted with respect to each other.

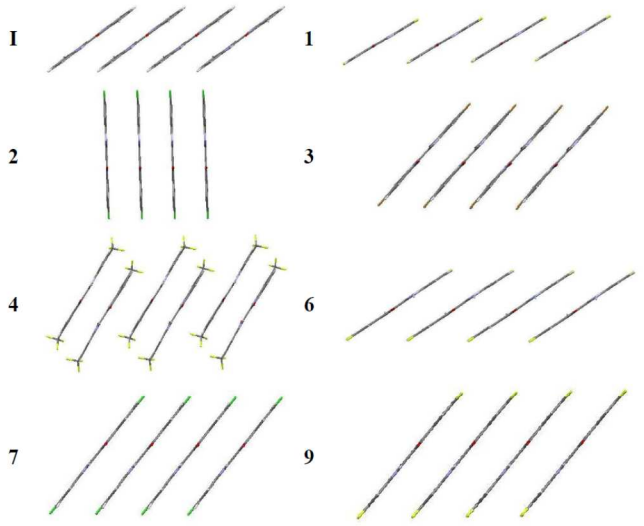

Figure 7. Arrangement of molecules in the crystals of some indigoids according to the single crystal X-ray diffraction data. Data for indigo (**I**) and compounds **2** and **3** are taken from literature.[19]

Assuming the orientation of the molecules on the dielectric substrate as revealed previously for the parent indigo,[8] compound **2** should have advanced charge transport properties due to the structure of its π-stacks and demonstrate advanced performances in OFETs. Indeed, this expectation agrees well with the transistor characteristics presented in Table 2.

Due to the presence of two bulky trifluoromethyl substituents in the 6,6'-bis(trifluoromethyl)indigo **4**, the molecules are arranged in pairs (Fig. 4). The distance between the molecules in the pair (3.42 Å) is considerably shorter compared to the distance between the pairs (3.92 Å). At the same time, the molecules in the pair are less shifted with respect to each other (shift angle ~108°) than the molecules belonging to the neighboring pairs (shift angle ~146°). These structural peculiarities result in the zig-zag shape of the π-stacks of indigoid **4** which should not favor the charge transport.

The crystal structures formed by indigoids in thin films were analyzed using grazing incident wide angle x-ray scattering (GIWAXS). The GIWAXS measurements allowed us to obtain few important parameters characterizing the surface structures of indigoids. The most intensive peak on the GIWAXS pattern reflects the π-stacking of the planar molecules in the film and reveals directly the characteristic d_π value. The azimuthal position of this peak was used to determine α angle. The tilt angle β was calculated as (90-α) degrees. The intermolecular distance was calculated as $d_m = d_\pi/\sin(\alpha)$ (Fig. 8). The simple relation between d_m and d_π is based on suggestion that the shift of the molecules along the short molecular axis direction is relatively low. This is proved by comparison of the corresponding unit cell parameters for the bulk and surface structures. It was found that the parameters are close for most of the compounds.

It has been shown that 5 out of 7 structurally characterized indigoids form new polymorphs in thin films (Table 3). The presence of two polymorphs was revealed for the thin films of indigoids **1**, **2**, **7** and **8**. The 6,6'-dibromoindigo **3** forms a single phase which has a different structure compared to the bulk one. It is surprising that this phase was not observed in the previous study of this material involving very similar technique.[9] The thin films of **4** and **6** also demonstrated single phases which, however, correspond to the bulk structures of these indigoids.

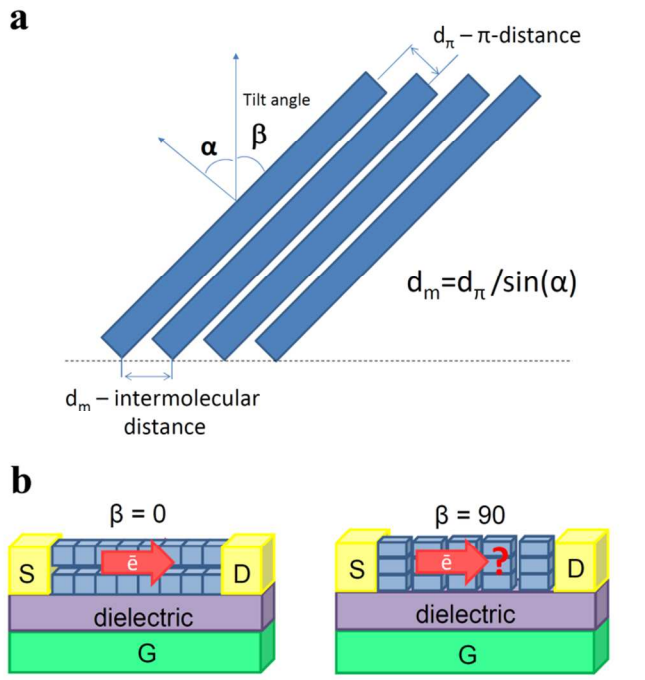

Figure 8 The meaning of the main parameters extracted from the GIWAXS measurements (a) and schematic illustration of the charge transport in OFETs based on the semiconductor films with tilt angles β=0 and β=90 degrees (b).

Table 3. Geometrical parameters determined for bulk and surface crystal structures of indigoids **1-9***

Comp.	Bulk structure			Surface structure*		
	Tilt angle β, deg.	Intermol. distance d_m, Å	π-distance, d_π, Å	Tilt angle β, deg.	Intermol. distance d_m, Å	π-distance, d_π, Å
1	56	6.06	3.40	5	3.61	3.58
2	4	3.40	3.36	0	3.60	3.57
3	40	4.01	3.34	67	3.66	3.37
4	30	3.69; 6.76	3.42; 3.92	The same as bulk structure		
5	N/A	N/A	N/A	90	N/A	3.40
6	57	6.03	3.37	The same as bulk structure		
7	29	4.32	3.34	59	4.22	3.6
8	N/A	N/A	N/A	56	4.3	3.57
9	42	4.39	3.30	36	4.43	3.58
Indigo	54	5.77	3.40	40	4.46	3.43

* - all indigoids formed the same polymorphs on TC and BCB with except for the parent indigo and **9** which showed epitaxial structures on TC only.

The 5,5',6,6'-tetrafluoroindigo **9** forms an epitaxial structure on TC with the intermolecular distance (d_m) of 4.43 Å (Fig. S6).

This value is very close to the distance between the neighboring linear aliphatic $CH_3(CH_2)_nCH_3$ chains known, for example, for (110) crystal plane in orthorhombic phase of polyethylene.[20] Very similar epitaxial structure was observed for the films of indigoid **9** grown on paraffin wax. At the same time, the structure of thin films of **9** grown on BCB dielectric corresponds to the bulk structure determined by the single crystal structure analysis. Thus, the tetrafluorindigo **9** behaves similarly to the parent indigo while undergoing epitaxial growth on aliphatic hydrocarbons.[11] However, in contrast to the parent indigo, two different crystal modifications of **9** formed on TC and BCB dielectrics showed very similar performances in OFETs (Table 2).

We note that tilting of molecules in the stack might affect significantly lateral charge transport required for efficient OFET operation. This effect is schematically illustrated in Fig. 8b. In the case of the zero tilt angle ($\beta=0^o$) the molecules stay perpendicularly to the substrate, while their stacks lay horizontally thus facilitating the charge transport between the source and drain electrodes in OFET. Other extreme case with $\beta=90^o$ is characterized by the vertically aligned π-stacks. The lateral charge transport depends in this case entirely on the hoping of charges between the neighboring stacks which is known to be inefficient. This explains why the films of dicyanoindigo **5** with the tilt angle $\beta=90^o$ did not reveal semiconductor behavior in OFETs. On the contrary, the surface structures of **1** (tilt angle $\beta=5^o$) and **2** ($\beta=0^o$) are the most favorable for the lateral charge transport. Indeed, these two indigoids exhibited the best performances in OFETs (Table 2) as compared to all other investigated semiconductors.

A correlation between the electrical performance of indigoids **1-9** in OFETs and angle β as a structural characteristic of their thin films is shown in Fig. 9.

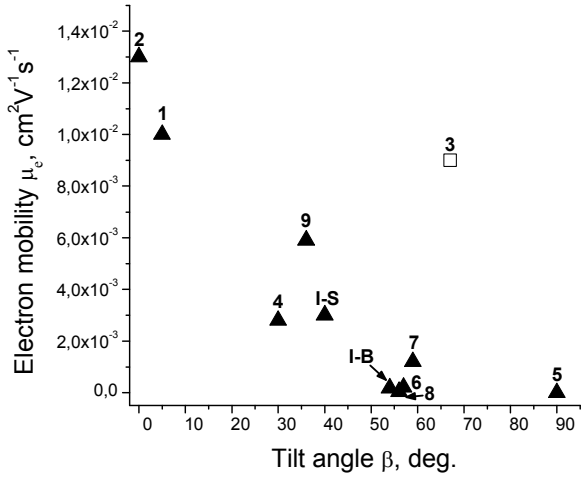

Figure 9. Correlation of the electron mobility with the tilt angle of the molecules in the surface structure revealed from the GIWAXS measurements. Compound numbers are given nearby the corresponding symbols; **I-S** and **I-B** correspond to the surface and bulk structures of pristine indigo, respectively.

Indeed, the electron mobility decreases rapidly with increase in the tilt angle. Surprisingly, all 5,5'-disubstituted indigoids showed rather big tilt angles in thin films which might explain their poor semiconductor performance. The presence of two bulky trifluoromethyl substituents in indigoid **4** damages its charge transport properties to some extent and prevents it from showing a higher mobility comparable to that of indigoid **9** with a similar tilt angle. The most unexpected was good electrical performance of indigoid **3** in spite of the relatively big tilt angle (β=67). However, remarkably short π-distance of 3.37 Å indicating strong intermolecular electronic coupling in the stacks facilitates charge transport and this effect counterbalances strong tilting of the molecules. The unusual surface structure of indigoid **3** deserves more detailed investigation in subsequent studies. Summarizing these results, we conclude that geometry of π-stacks in semiconductor thin films is a factor of crucial importance which affects dramatically their performance in OFETs.

The observed drastically different performance of indigoids **3** and **4** on TC and BCB dielectrics was also addressed using the GIWAXS data. Thus, the thin films of **4** grown on BCB did not reveal the presence of any crystalline phase (Fig. S7). It is very likely that BCB prevents substrate-induced crystallization of indigoid **4** due to non-periodical surface structure and the resulting disordered semiconductor films do not show any transistor characteristics. At the same time, the crystalline films of **4** grown on TC demonstrated reasonably good operation in OFETs. The observed considerable difference in the ordering of thin films of 6,6'-dibromoindigo **3** grown on TC (highly ordered) and BCB (poorly ordered) account for their performance in OFETs. Thus, TC and BCB dielectrics influence on the local ordering of the grown above semiconductor layers thus affecting their electrical characteristics. These examples suggest that supramolecular interactions between the semiconductor and dielectric deserve a special attention.

The indigoid-based semiconductors are considered as highly promising materials for designing OFETs with excellent operational stability under ambient conditions.[9-10] According to the literature, a stable n-channel OFET operation under ambient conditions is achieved when anion species formed by the reduced semiconductor molecules do not react with oxygen and moisture.[21] It is known that water and oxygen can undergo the following major reduction pathways:

$$2\ H_2O + 2\ \bar{e} \rightarrow H_2 + 2\ OH^- \quad (1)$$
$$O_2 + \bar{e} \rightarrow O_2^{\cdot-} \quad (2)$$
$$2\ H_2O + O_2 + 4\ \bar{e} \rightarrow 4\ OH^- \quad (3)$$

Typically, organic molecules having higher electron affinities compared to the oxygen and water form anion species which are fairly stable under ambient conditions. The electrochemical potentials corresponding to the reactions (1) and (3) were reported to be *ca.* -0.66 V and +0.57 V *vs.* standard calomel electrode (SCE), respectively.[21] For the oxygen to superoxide reduction in aprotic media (reaction (2)), the half-wave

potentials of-0.86 V *vs.* SCE (onset at *ca.* -0.75 V vs. SCE) in anhydrous acetonitrile and -0.70 V *vs.* Ag/AgCl (onset at *ca.* -0.60 V vs. Ag/AgCl) in an ionic liquid were reported.[22] Using standard equations, one can estimate that reduction potentials of water (equation (1)) and oxygen (equation (2)) correspond to *ca.*-4.1 eV and-4.0 eV (based on the onset value) in the Fermi energy scale, respectively.[17] Therefore, organic semiconductor should have its LUMO energy at least below -4.1 eV to be stable against moisture and oxygen separately (equations (1) and (2) above). It is notable that the redox process depicted by the equation (3) is characterized by the Fermi energy of ca. -5.3 eV. Therefore simultaneous action of oxygen and water can damage the n-type operation of any material with LUMO energy above -5.3 eV. Fortunately, the concentrations of oxygen and moisture in the semiconductor layer are very low, therefore, the redox process outlined by the equation (3) does not play important role at least when the devices are exposed to air for a relatively short time. Therefore, one can practically observe air-stable n-type operation of OFETs based on the materials with LUMO energy below -4.1 eV. This hypothesis was confirmed in a number of experimental studies.[23]

It was reported previously that OFETs comprising 6,6'-dibromoindigo **3** as semiconductor revealed completely "air-stable operation" due to its low lying LUMO energy of -4.0 eV.[9] However, this result contradicts to the electrochemical data obtained in this work and presented in Table 1. Indeed, all indigoids bearing chlorine and bromine substituents (**2**, **3**, **7**, **8**) exhibit virtually identical reduction waves and have the same LUMO energy levels as parent non-substituted indigo. The absolute LUMO energy of *ca.* -3.9 eV was estimated for indigo and its chlorinated and brominated derivatives using the approach presented in the literature.[17]

In order to avoid any mistakes arising from the conversion of the electrochemical potentials to the Fermi energy scale, we investigated a well-known reference material N,N'-didodecyl-3,4,9,10-perylenedicarboximide (C12PDI) under exactly the same experimental conditions as used for indigoids **1-9**. The C12PDI revealed almost the same onset of the first reduction band as parent indigo and aforementioned halogenated indigoids (Fig. S7). It is known that such dialkylsubstituted PDIs have LUMO of *ca.* -3.8 to -4.0eV and do not show air-stable OFET performances.[24] Introducing two cyano groups at the bay region of PDIs lowers their LUMO energy down to -4.3 eV which improves strongly ambient stability of OFETs,[23,25] though some noticeable degradation can still occur.[26]

The obtained results suggest that OFETs comprising 6,6'-dibromoindigo **3** as semiconductor can hardly show an air-stable operation. Indeed, experimental investigation of OFETs comprising **1**, **3**, or **7** as semiconductors revealed their rapid degradation under ambient conditions (25-27 ^{o}C, 30-35% RH, continuous storage and periodic measurement in air) within few hours. Surprisingly, the devices comprising 6,6'-dichloroindigo **2** were somewhat more stable and degraded in few days. The observed minor improvement in the ambient stability of **2** might be related to its dense molecular packing in crystal phase which might slow down the diffusion of moisture and oxygen.

The OFETs comprising indigoids **4** and **9** demonstrated a superior ambient stability as it is shown in Fig. 10. In particular, the electron mobility measured for **9** decreases within the first few days and then stabilizes at some reasonable values. Thus, the most stable OFETs operated in air for more than 70 days (when measurements were intentionally terminated). The storage of the air-exposed devices inside argon glove box within few days recovered (partially or completely) their initial electrical characteristics.

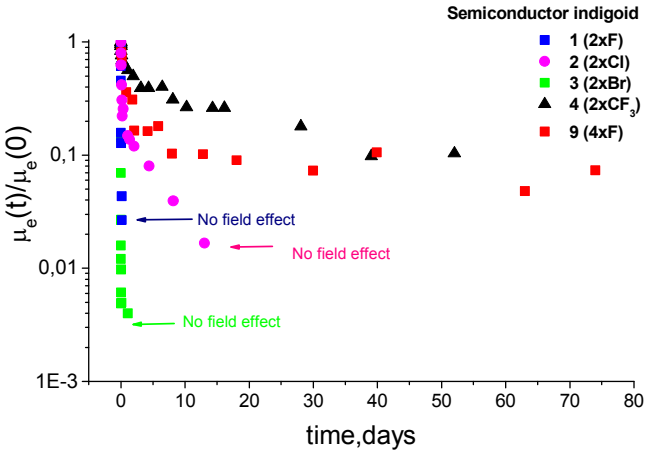

Figure 10. Relative ambient stability of n-channel OFETs comprising different indigoid semiconductors (storage and measurements in air)

We emphasize that the experimental data on the ambient operation stability of OFETs comprising different indigoids correlate well with their electrochemical properties presented in Table 1. Indeed, compounds **4** and **9** possessing the lowest LUMO energy levels (except for 6,6'-dicyanoindigo **5** and 5,5'-difluoroindigo **6**, which did not reveal good semiconductor behavior in OFETs) showed also the highest ambient stabilities. Indigoid **9** was much more stable compared to **4** presumably due to a denser crystal packing preventing fast diffusion of oxygen and moisture. We emphasize that OFETs based on indigoid **9** operate in air reasonable well even after 70 day exposure. This reflects a dramatic improvement in the ambient stability as compared to dihalogenated indigoids **1-3**.

The deterioration of the OFET characteristics observed for both semiconductors **4** and **9** under ambient conditions can be expected since their LUMO levels are still somewhat higher than required for the real air-stable operation. It is reasonable to assume that the presence of multiple fluorine atoms in the molecular structures of **4** and **9** increases their hydrophobicity. Moisture is known to be much more aggressive agent compared to oxygen,[23] therefore preventing water diffusion to the semiconductor layer should improve significantly the device stability. Similar approach was used to improve the ambient stability of n-type OFETs previously.[27]

On the base of the aforementioned experimental results and considerations, we can propose the structures of 4,4',6,6',7,7'-hexafluoroindigo, 5,5',6,6',7,7'-hexafluoroindigo 4,4',5,5',6,6',7,7'-octafluoroindigo, and 5,5',6,6'-tetrakis-

(trifluoromethyl)indigo as promising n-type semiconductors which should enable truly air-stable operation of OFETs. The latter compound might exhibit low charge carrier mobility due to the presence of bulky substituents. The synthesis of these compounds and experimental investigation might be pursued in future. However, there is some concern regarding the unexpected biological activity of these strongly functionalized indigoids and especially regarding their biodegradability. These aspects have to be addressed in future also for some indigoids presented in this work.

Conclusions

Indigo and its functional derivatives represent a promising group of semiconductor materials for organic electronics. It has been shown that chemical derivatization influences significantly optical and electronic properties of indigoids as well as their electrical performance in OFETs. In particular, 5,5'-disubstituted indigoids demonstrate inferior performances compared to the 6,6'-disubstituted analogs. It is notable that electron deficient substituents inhibit hole transport in indigoid films, while electron transport remains almost unaffected. Thus, 6,6'-dibromoindigo shows ambipolar transport which becomes strongly unbalanced going to chlorinated and fluorinated analogs, while indigoids bearing two CF_3 groups (**4**) or four fluorine atoms (**9**) demonstrate purely n-type behavior.

The experimental data obtained in this work revealed that ambient stability of OFETs based on indigo and 6,6-dibromoindigo (Tyrian purple) was severely overestimated in the previous publications.[8-10] According to our results, these devices degrade in air almost completely within few hours. However, this problem was partially solved by introducing strong electron withdrawing substituents such as two CF_3 groups or four fluorine atoms which lowered the LUMO energy of the indigo core and improved dramatically the stability of n-channel OFETs under ambient conditions. The lifetime of the continuously stored and periodically measured in air OFETs based on 6,6'-bis(trifluoromethyl)indigo **4** and 5,5',6,6'-tetrafluoroindigo **9** exceeded 60 days.

In order to reach truly air-stable device operation, it is necessary to design some novel indigoids with further decreased LUMO energy levels down to at least -4.3 eV. This can be potentially fulfilled for perfluorinated indigo or 5,5',6,6'-tetrakis(trifluoromethyl)indigo. However, going this way we should keep in mind that so strong chemical derivatization of indigo will change not only the optoelectronic characteristics of this material, but also its biological properties (particularly, acute toxicity) and biodegradability. Therefore, newly designed materials have to be adequately assessed before recommending them for sustainable electronics applications.

Experimental

Materials and instrumentation

Indigo and tetracontane were purchased from Sigma-Aldrich. Other reagents and solvents were purchased from Acros Organics. Toluene and chlorobenzene were purified using standard distillation. Tetracontane and mesitylene were used as received. The dielectric BCB was obtained under the trade name CYCLOTENE 4024 resin as a product of The Dow Chemical Company.

FTIR spectra were measured in KBr pellets using Perkin Elmer Spectrum BX instrument. ESI MS spectra were measured using Shimadzu LCMS 2020. UV-VIS spectra were obtained using Avantes AvaSpec-2048 fiber optic spectrometer for solutions of indigoids in 1,2-dichlorobenzene heated up to 50 degrees.

Synthesis of indigoids and their spectral characteristics

The indigoids **1-8** were synthesized using previously reported procedures.[12] The indigoid **9** was prepared using alternative procedure.[13] Purification of the prepared compounds was achieved using multistep temperature gradient vacuum sublimation. Indigoids **1-3**, **5** and **9** were sublimed at 220-240 C under the pressure of $1 \cdot 10^{-2}$ mm Hg. Indigoids **6-8** were sublimed at 240-260 ^{o}C under the pressure of $1 \cdot 10^{-2}$ mm H. Indigoid **4** sublimed at 200-220 ^{o}C under the same pressure. Each compound was sublimed at least four times before evaluation in OFETs. The spectral characteristics of the known compounds were identical to the reported in literature.[14]

Compound 1. FT-IR (KBr): 3384, 1636, 1618, 1578, 1442, 1388, 1316, 1282, 1202, 1160, 1082, 1060, 912, 850, 814, 766, 694, 642, 600, 532, 482 cm^{-1}. ESI-MS $[C_{16}H_7F_2N_2O_2]^-$ m/z = 298. Chemical analysis (%) calcd for $C_{16}H_8F_2N_2O_2$: C 64.43, H 2.70, F 12.74; N 9.39; found C 64.21, H 2.65, F 12.42, N 9.16.

Compound 2. FT-IR (KBr): 3342, 1684, 1644, 1622, 1442, 1388, 1320, 1286, 1168, 1112, 618 cm^{-1}. ESI-MS $[C_{16}H_7Cl_2N_2O_2]^-$ m/z = 329. Chemical analysis (%) calcd for $C_{16}H_8Cl_2N_2O_2$: C 58.03, H 2.43, N 8.46; found C 58.17, H 2.32, N 8.39.

Compound 3. FT-IR (KBr): 3382, 1628, 1606, 1436, 1384, 1312, 1280, 1194, 1144, 1068, 1048, 896, 590, 526 cm^{-1}. ESI-MS $[C_{16}H_7Br_2N_2O_2]^-$ m/z=419. Chemical analysis (%) calcd for $C_{16}H_8Br_2N_2O_2$: C 45.75, H 1.92, N 6.67; found C 45.64, H 1.74, N 6.69.

Compound 4. FT-IR (KBr): 3342, 1642, 1626, 1502, 1448, 1400, 1328, 1236, 1150, 1134, 1052, 918, 878, 834, 772, 702 cm^{-1}. ESI-MS $[C_{18}H_7F_6N_2O_2]^-$m/z = 397. Chemical analysis (%) calcd for $C_{18}H_8F_6N_2O_2$: C 54.28, H 2.02, F 28.62; N 7.03; found C 54.04, H 2.13, F 28.77, N 6.75.

Compound 5. FT-IR (KBr): 3342, 1684, 1644, 1622, 1442, 1388, 1320, 1286, 1168, 1112, 618 cm^{-1}. ESI-MS $[C_{18}H_8N_4O_2]^-$m/z = 312. Chemical analysis (%) calcd for $C_{18}H_8N_4O_2$: C 69.23, H 2.58, N 17.94; found C 68.97, H 2.61, N 17.64.

Compound 6. FT-IR (KBr): 3286, 1624, 1482, 1458, 1314, 1262, 1182, 1108, 1054, 822, 684 cm^{-1}. ESI-MS $[C_{16}H_7F_2N_2O_2]^-$ m/z = 298. Chemical analysis (%) calcd for $C_{16}H_8F_2N_2O_2$: C 64.43, H 2.70, F 12.74; N 9.39; found C 64.72, H 2.43, F 12.51, N 9.10.

Compound 7. FT-IR (KBr): 3280, 1628, 1608, 1462, 1448, 1306, 1258, 1186, 1120, 1046, 824, 782, 642, 594 cm^{-1}. ESI-MS $[C_{16}H_7Cl_2N_2O_2]^-$m/z = 329. Chemical analysis (%) calcd

for $C_{16}H_8Cl_2N_2O_2$: C 58.03, H 2.43, N 8.46; found C 57.77, H 2.37, N 8.37.

Compound 8. FT-IR (KBr): 3280, 1628, 1606, 1458, 1442, 1386, 1302, 1256, 1184, 1118, 1078, 1042, 884, 822, 780, 616, 594 cm^{-1}. ESI-MS $[C_{16}H_7Br_2N_2O_2]^-$ m/z = 419. Chemical analysis (%) calcd for $C_{16}H_8Br_2N_2O_2$: C 45.75, H 1.92, N 6.67; found C 45.90, H 1.82, N 6.65.

Compound 9. FT-IR (KBr): 3302, 1634, 1596, 1472, 1384, 1336, 1316, 1214, 1144, 1120, 1038, 884, 844, 778, 744, 668, 624 cm^{-1}. ESI-MS $[C_{16}H_5F_4N_2O_2]^-$ m/z = 333. Chemical analysis (%) calcd for $C_{16}H_6F_4N_2O_2$: C 57.50, H 1.81, F 22.74; N 8.38; found C 57.19, H 2.02, F 22.49, N 8.53.

X-ray crystallography

Synchrotron X-ray data for compounds **1**, **4**, **6**, and **9** were collected at 100 K at the BL14.2 at the BESSY storage ring (PSF, Free University of Berlin, Germany) using a MAR225 CCD detector. Data collection for compound **7** was carried out at 100 K with an image-plate diffractometer (IPDS, Stoe). Crystallographic data along with some details of data collection and structure refinements are presented in Table S6. The structures were solved and anisotropically refined with SHELX package.[28] In the crystal structures **6** and **7**, hydrogen atoms were refined isotropically, whereas in other crystal structures H atoms were placed in geometrically calculated positions and refined in a riding mode. CCDCs 991835 (**1**), 991836 (**4**), 991837 (**6**), 991838 (**7**), and 991839 (**9**) contain the supplementary crystallographic data for this paper. These data can be obtained free of charge from The Cambridge Crystallographic Data Centre via www.ccdc.cam.ac.uk/data_request/cif.

Cyclic voltammetry measurements

The cyclic voltammetry measurements were performed for thin films (150-160 nm thick) of indigo and its derivatives deposited on glassy carbon disc electrode (working electrode, d=5 mm, BAS Inc.) by thermal evaporation in vacuum ($5 \cdot 10^{-5}$ mbar) with the rate of 1.2 Å/s. The measurements were performed in a three-electrode electrochemical cell using 0.1 M solution of Bu_4NPF_6 in acetonitrile as supporting electrolyte, platinum wire as a counter electrode and a silver wire immersed in 0.01 M solution of $AgNO_3$ in 0.1 M TBAP (CH_3CN) as a reference Ag/Ag^+ electrode (BAS Inc.). Ferrocene was used as internal reference. The electrolyte solution was purged with argon before the measurements. The voltammograms were recorded using ELINS P-30SM instrument at room temperature with a potential sweep rate of 50 mV/s.

OFET fabrication

A 1 mm wide and 200 nm thick aluminum gate electrode was deposited by thermal evaporation onto 1.5 × 1.5 cm^2 glass slides. It was subsequently anodized by immersing in a citric acid solution (0.2 g per 100 mL) in a potentiostatic regime at 10 V to achieve a formation of uniform AlO_x coating. Afterwards, the samples were rinsed with deionized water and dried in an oven at 80 °C for 30 min. Organic dielectric coatings were deposited immediately after taking the samples out from the oven.

Tetracontane TC (Aldrich) was dissolved in toluene to achieve a total material concentration of 1.5 mg/ml. The resulting solution was spin-coated onto the dried Al/AlO_x electrodes at 3000 rpm.

Benzocyclobutene derivative BCB was deposited from a commercial CYCLOTENE 4024 resin solution diluted with mesitylene in 1:100 v/v ratio. The obtained solution was spin-coated onto the Al/AlO_x substrates at 1500 rpm. The resulting coatings were annealed overnight on a hot plate at 280 °C inside argon glove box.

The capacitances of the dielectrics were measured at 1-10 MHz frequency for conventional MIM devices. The obtained values were 350-370 nF/cm^2 for bare AlO_x, 250-270 nF/cm^2 for AlO_x/TC and 70-80 nF/cm^2 for AlO_x/BCB.

Semiconductor films of indigoids were grown on the organic dielectric coating by thermal evaporation from a resistively heated quartz crucible at a pressure of 2×10^{-6} mbar at the rate of 0.6 Å/s. The typical thickness of the indigoid films was 100 nm. Silver or gold source and drain electrodes (typically 100 nm) were evaporated through a shadow mask (L = 50 μm, W = 2 mm) at a pressure of 2×10^{-6} mbar. Transistor characterization was carried out inside an argon glove box with <1 ppm O_2 and <1 ppm H_2O. The transfer and output characteristics were recorded using Kethley 2612A instrument with LabTracer software.

GIWAXS measurements

The samples were prepared in the same way as in the case of OFET fabrication using silicon slides as substrates. A set of samples with the thickness of indigoid films varied between 70 nm and 500 nm was prepared for every compound on both investigated dielectric coatings (TC and BCB). GIWAXS measurements were performed using XeuSS SAXS/WAXS (Xenocs, France) machine coupled to GeniX3D generator (λ =1.54 Å). The 2D data were collected with the incidence angle 0.2° using Rayonix HS170 CCD detector (pixel size 132x132 μm) with sample to detector distance approx. 18cm. The minimum projection method for series of images was used to reduce background noise. The modulus of the scattering vector s (s = 2sinθ/λ, where θ is the Bragg angle) was calibrated using seven diffraction orders of silver behenate powder. The indexing of 2D-GIWAXS patterns was performed in home-made routine written in Igor Pro software.

AFM and SEM microscopy and optical spectroscopy

Atomic force microscopy (AFM) and scanning electron microscopy (SEM) images were typically measured from the channels of the fabricated OFETs after electrical I-V characterization. NTEGRA PRIMA instrument (NT MDT, Russia) was used to obtain the AFM images. SEM images were obtained on a Zeiss LEO SUPRA 25 instrument.

The optical spectroscopy studies were performed for 300 nm thick indigoid films grown on the borosilicate glass slides. The

absorption spectra were measured using Avantes 2048 dual-channel fiber spectrometer equipped with a sample holder installed inside an argon glove box.

Acknowledgements

This work was supported by RFBR (13-03-01170a), the Russian Ministry of Science and Education (project for financial support of leading scientists №11.G34.31.0055), and the Russian President Science Foundation (МК-5260.2014.3).

Notes and references

[a] IPCP RAS, Semenov Prospect 1, Chernogolovka, 142432, Russia. Fax: +7 496515-5420; Tel: +7 496522 1418; E-mail: troshin2003@inbox.ru
[b] Department of Chemistry, Moscow State University, Leninskie gory, Moscow, 119991, Russia
[c] M. V. Lomonosov Moscow State University, Faculty of Fundamental Physical and Chemical Engineering, GSP-1, 1-51 Leninskie Gory, Moscow, 119991, Russia
[d] Institute of Energy Problems for Chemical Physics (Branch) RAS, Semenov Prospect 1, Chernogolovka, 142432, Russia
[e] Institut de Science des Matériaux de Mulhouse, LRC CNRS 7228, 15 rue Jean Starcky, BP 2488, Mulhouse CEDEX, 68057, France

Electronic Supplementary Information (ESI) available: Optical absorption spectra for solutions and thin films, cyclic voltammograms, transfer and output characteristics of OFETs, AFM and SEM images, illustration of the geometrical parameters presented in Table 3, selected GIWAXS and X-ray single crystal diffraction data. See DOI: 10.1039/b000000x/

1. N. T. Kalyani and S. J. Dhoble, *Renewable and sustainable energy reviews*, 2012, **16**, 2696; T. Yamada and Y. Tsubata, *J. Synth. Org. Chem. Jap*., 2012, **70**, 473.
2. H. Klauk Ed., *Organic Electronics II: More Materials and Applications. WILEY VCH,* 2012.
3. M. Irimia-Vladu, *Chem. Soc. Rev*., 2014, **43**, 588.
4. M. Irimia-Vladu, P. A. Troshin, M. Reisinger, L. Shmygleva, Y. Kanbur, G. Schwabegger, M. Bodea, R. Schwödiauer, A. Mumyatov, J. W. Fergus, V. Razumov, H. Sitter, N. S. Sariciftci and S. Bauer, *Adv. Funct. Mater*., 2010, **20**, 4069.
5. M. Irimia-Vladu, P. A. Troshin, M. Reisinger, G. Schwabegger, M. Ullah, R. Schwödiauer, A. Mumyatov, M. Bodea, J. W. Fergus, V. Razumov, H. Sitter, S. Bauer and N. S. Sariciftci, *Organic Electronics*, 2010, **11**, 1974; M. Irimia-Vladu, P. A. Troshin, G. Schwabegger, M. Bodea, R. Schwödiauer, J. W. Fergus, V. F. Razumov, S. Bauer, N. S. Sariciftci. Proc. SPIE 7778, Organic Field-Effect Transistors IX, 777803.
6. K. H. Ferber, *J. Environ. Pathol. Toxicol. Oncol*., 1987, **7**, 73; Reports of the Scientific Committee for Food. 13th Series., SCF 1983; http://ec.europa.eu/food/fs/sc/scf/reports_en.html.
7. Y. Hiroyuki, *Organic transistor. JP*, 2008-098454A.
8. M. Irimia-Vladu, E. D. Głowacki, P. A. Troshin, G. Schwabegger, L. Leonat, D. K. Susarova, O. Kryshtal, G. Schwabegger, M. Ullah, Y. Kanbur, M. A. Bodea, V. Razumov, H. Sitter, S. Bauer and N. S. Sariciftci, *Adv. Mater*., 2012, **24**, 375.
9. E. D. Głowacki, L. Leonat, G. Voss, M.-A. Bodea, Z. Bozkurt, A. M. Ramil, M. Irimia-Vladu, S. Bauer and N. S. Sariciftci., *AIP Advances*, 2011, **1**, 042132; Y. Kanbur, M. Irimia-Vladu, E. D. Glowacki, G. Voss, M. Baumgartner, G. Schwabegger, L. Leonat, M. Ullah, H. Sarica, S. Erten-Ela, R. Schwodiauer, H. Sitter, Z. Kucukyavuz, S. Bauer and N. S. Saricifci, *Org. Electron*., 2012, **13**, 919.
10. E. D. Głowacki, G. Voss and N. S. Sariciftci. *Adv. Mater.* 2013, ***25***, 6783.
11. D. V. Anokhin, L. I. Leshanskaya, D. K. Susarova, N. N. Dremova, E. V. Shcheglov, D. A. Ivanov, V. F. Razumov and P. A. Troshin, *Chem. Commun*. 2014, 10.1039/C4CC02431A.
12. J. Harley-Mason, J. Chem. Soc., 1950, 2907; G. Voss and H. Gerlach, *Chem. Ber*., 1989, **122**, 1199.
13. P. Friedländer, *Monatch. Chem*., 1909, **30**, 247-253; J. Wolk, A. Frimer, *Molecules*, 2010, **15**, 5561.
14. Y. Tanoue, K. Sakata, M. Hashimoto, M. Hamada, N. Kai and T. Nagai, *Dyes and Pigments*, 2004, **62**, 101; H. J. Gerlach, patent DE 3910648A1, 1990.
15. P. W. Sadler, *J. Org. Chem*., 1956, **21**, 316; M. Lamsabhi, C. A. Escobar and P. Perez, *J. Phys. Org. Chem*., 2005, **18**, 1161.
16. A. Eisfeld, J.S. Briggs, *Chem. Phys*. 2006, **324**, 376.
17. C. M. Cardona, W. Li, A. E. Kaifer, D. Stockdale and G. C. Bazan, *Adv. Mater*., 2011, **23**, 2367.
18. S. Y. Yang, K. Shin and C. E. Park, *Adv. Funct. Mater*. 2005, **15**, 1806.
19. H. von Eller, *Bull. Soc. Chim. Fr*., 1955, 1433; E. A. Gribova, G. S. Zhdanov and G. A. Gol'der, *Kristallografiya (Russ.) (Crystallogr. Rep.)*, 1956, **1**, 53; P. Susse and A. Wolf, *Naturwissenschaften*, 1980, **67**, 453; P. Susse, M. Steins and V. Kupcik, *Z. Kristallogr*., 1988, **184**, 269; F. Kettner, L. Huter, J. Schafer, K. Roder, U. Purgahn and H. Krautscheid, *Acta Crystallogr., Sect. E: Struct. Rep. Online*, 2011, **67**, o2867; P. Susse and C. Krampe, *Naturwissenschaften*, 1979, **66**, 110; S. Larsen and F. Watjen, *Acta Chem. Scand. A*, 1980, **34**, 171; P. Susse and R. Wasche, *Naturwissenschaften*, 1978, **65**, 157.
20. P.H. Geil, Polymer Single Crystals, Krieger Pub Co; 1st Ed., London, 1973
21. D. M. de Leeuw, M. M. J. Simenon, A. R. Brown and R. E. F. Einerhand, *Synthetic Metals,* 1997, **87**, 53.
22. I. M. AlNashef, M. L. Leonard, M. C. Kittle, M. A. Matthews and J. W. Weidner, *Electrochemical and Solid-State Letters*, 2001, **4**, D16; D. T. Sawyer, A. Sobkowiak, and J. L. Roberts, *Electrochemistry for Chemists*, 1995, 2nd ed., Chap. **9**, Wiley Interscience, New York.
23. T. D. Anthopoulos, G. C. Anyfantis, G. C. Papavassiliou and D. M. de Leeuw, *Appl. Phys. Lett*. 2007, **90**, 122105; T. D. Anthopoulos, F. Kooistra, H. J. Wondergem, D. Kronholm, J. C. Hummelen and D. M. de Leeuw, *Adv. Mater*,. 2006, **18**, 1679.
24. J. H. Oh, Y.-S. Sun, R. Schmidt, M. F. Toney, D. Nordlund, M. Konemann, F. Wurthner and Z. Bao, *Chem. Mater*., 2009, **21**, 5508; Y. Wen, Y. Liu, C.-A. Di, Y. Wang, X. Sun, Y. Guo, J. Zheng, W. Wu, S. Ye and G. Yu, *Adv. Mater*., 2009, **21**, 1631.
25. B. A. Jones, M. J. Ahrens, M. H. Yoon, A. Facchetti, T. J. Marks and M. R. Wasielewski, *Angew. Chem*., Int. Ed. 2004, **43**, 6363.
26. T. Weitz, K. Amsharov, U. Zschieschang, E. Barrena Villas, D. K. Goswami, M. Burghard, H. Dosch, M. Jansen, K. Kern and H. Klauk, *J. Am. Chem. Soc*., 2008, **130**, 4637.
27. H. E. Katz, A. J. Lovinger, J. Johnson, C. Kloc, T. Siegrist, W. Li, Y.-Y. Lin and A. Dodabalapur, *Nature*, 2000, **404**, 478.

28. G. M. Sheldrick, *Acta Cryst. A* 2008, **64**, 112.

